THE ASTROPHYSICAL JOURNAL, 180:31–53, 1973 February 15

MOLECULAR CLOUDS IN W49 AND W51

N. Z. SCOVILLE*
Department of Astronomy, Columbia University
AND
P. M. SOLOMON
School of Physics and Astronomy, University of Minnesota
Received 1972 June 30; revised 1972 September 28

ABSTRACT

Radio observations of six molecular lines have been obtained in the W49 and W51 H II region sources as part of an investigation of the physical conditions in molecular clouds and the relationship of these clouds to the H II regions. The principal observations are maps with 4′ spacing of the 6-cm formaldehyde (H_2CO) absorption and strip maps with 1′ spacing of carbon monoxide (CO, $J = 1 \rightarrow 0$) emission at 2.6 mm. A few selected positions were also observed in ^{13}CO and $C^{18}O$ as well as the carbon monosulfide lines (CS, $3 \rightarrow 2$ and $2 \rightarrow 1$) at 2 and 3 mm.

Seven distinct clouds are found, and five of these are associated with or near H II regions. The molecular clouds are all much larger than the H II regions; one near W51 (at 65 km s^{-1}) extends over an area containing at least three H II regions and appears as a self-absorption feature in CO. The mass of three of these molecular clouds is estimated to be at least 10^4–10^5 $M_\odot$, 10 times as great as the ionized regions. Average hydrogen molecule densities, over the entire clouds, are about 200–1000 cm^{-3}; but near the H II regions there are probably compact, high-density ($\gtrsim 10^6$ cm^{-3}) molecular regions which are responsible for the high-excitation lines of CS.

The excitation temperature of the 6-cm H_2CO transition in two clouds in the direction of W49A is estimated to be $1.76° \pm 1.2°$ K. The large velocity difference between these clouds and the H II region and the narrowness of the lines suggest that the clouds are dark nebulae and unrelated to W49A; however, there is H_2O maser emission at the velocities of the dark cloud lines suggesting that some of the maser emission may be from foreground objects.

Subject headings: molecules, interstellar — nebulae — radio lines — star formation

I. INTRODUCTION

Initial surveys of 6-cm formaldehyde (H_2CO) and 2.6-mm carbon monoxide (CO) lines have demonstrated their great potential for structural studies of dense, interstellar clouds. The ubiquity and short wavelengths of these lines permit high-angular-resolution observations of most clouds having more than a few magnitudes of visual extinction. Moreover, the CO line is always seen in emission, and the H_2CO line, in absorption; they therefore provide complementary data vis-à-vis the spatial relationship of the continuum radiation sources and molecular clouds. In the vicinity of the galactic center, H_2CO (Scoville, Solomon, and Thaddeus 1972) and CO (Solomon *et al.* 1972*b*) observations reveal several molecular clouds with high densities ($\gtrsim 10^3$ H cm^{-3}) and large masses (10^4–10^6 $M_\odot$). The most massive cloud in the galactic center is associated with a compact H II region (Sgr B2), and we inquire whether similar clouds exist near compact H II regions outside the galactic center. Away from the complexities of the galactic-center region, it should also be easier to study these clouds and investigate their relationship to the H II regions.

* Present address: School of Physics and Astronomy, University of Minnesota, Minneapolis, Minnesota.

Here we report the results of H_2CO, CO, and CS observations of the galactic radio sources W49 and W51. These regions were selected because broad molecular lines, similar to those seen in the galactic center, had previously been detected there (Zuckerman *et al.* 1970; Penzias, Jefferts, and Wilson 1971*a*) and the H II regions themselves have been the focus of many continuum and recombination-line studies. Both regions are completely obscured at visual wavelengths and were first detected in Westerhout's (1958) 22-cm survey. Investigations with high angular resolution have shown that the thermal emission from these sources comes mostly from compact H II regions and that nonthermal emission is also present.

The W49 source (fig. 1*a*) consists of a thermal component W49A (G43.2−0.0) and, 12′ to the east, a nonthermal component W49B (G43.3−0.2). Analysis of the W49A spectrum (Mezger, Schraml, and Terzian 1967) and high-resolution aperture-synthesis observations (Wynn-Williams 1969) show that the H II region consists of several small condensations of high electron density ($n_e > 10^4$ cm^{-3}), embedded in a more extended and lower density ($n_e \sim 200$ cm^{-3}) region. This model is further supported by the 109α and 137β hydrogen recombination lines from W49A (Gordon and Wallace 1971). The distance of W49A, determined from its recombination-line velocity, is 14.1 kpc, and the mass of ionized gas is between $2 \times 10^3\ M_\odot$ and $10^4\ M_\odot$.

The W51 region is more complex than W49 (fig. 1*b*). The most intense component at 6 cm is G49.5−0.4, but there are at least six other thermal sources all superposed on a weak nonthermal background (Wilson *et al.* 1970; Shaver 1969). Interferometric observations at 11 cm show that G49.5−0.4 contains several very high brightness knots (Miley *et al.* 1970), perhaps similar to those found in W49A. The recombination-line velocities of all the W51 H II regions except G48.6+0.0 (not shown in fig. 1*b*) places them near the tangency point at $l = 49°$—that is, between 6.5 and 8 kpc from the Sun. The mass of G49.5−0.4 is $3.7 \times 10^3\ M_\odot$, and the masses of the other H II regions shown in figure 1*b* are between $2.8 \times 10^2\ M_\odot$ and $5.2 \times 10^3\ M_\odot$.

Observations of nonthermal OH emission in W49 and W51 show a close spatial and velocity coincidence between the OH clouds and several of the component H II regions (Rogers *et al.* 1966; Raimond and Eliasson 1969). Broad formaldehyde absorption lines have also been detected in the same directions (Zuckerman *et al.* 1970; Whiteoak and Gardner 1970); but to clarify the relationship between the molecular clouds and H II regions, it is clear that the molecular lines must be mapped at least over the full angular extent of the radio sources.

Our 6-cm H_2CO observations were made on a grid with 4′ spacing covering W49A and most of W51; 2.6-mm CO observations near the 6-cm peak of W49A were spaced by 1′ in the shape of a cross. The positions of these observations are shown superposed on the 6-cm continuum brightness contours in figure 1. Penzias *et al.* (1971*a*) have already mapped the CO lines near the peak (G49.5−0.4) in W51 to which we have added a few outlying points. Observations of ^{13}CO, $C^{18}O$, and CS ($J = 2 \rightarrow 1$ and $3 \rightarrow 2$) were also made at a few positions suggested by the CO and H_2CO observations (generally near the continuum peaks).

II. OBSERVATIONS AND ANALYSIS

a) H_2CO

The formaldehyde observations were made in 1971 April with the 140-foot (43-m) antenna and a cooled 6-cm parametric amplifier of the National Radio Astronomy Observatory (NRAO)[1] in Green Bank, West Virginia. The measured half-power beamwidth (HPBW) and beam efficiency (η) of the antenna are 6′.6 and 0.8 at 6 cm,

[1] Operated by Associated Universities, Inc., under contract with the National Science Foundation.

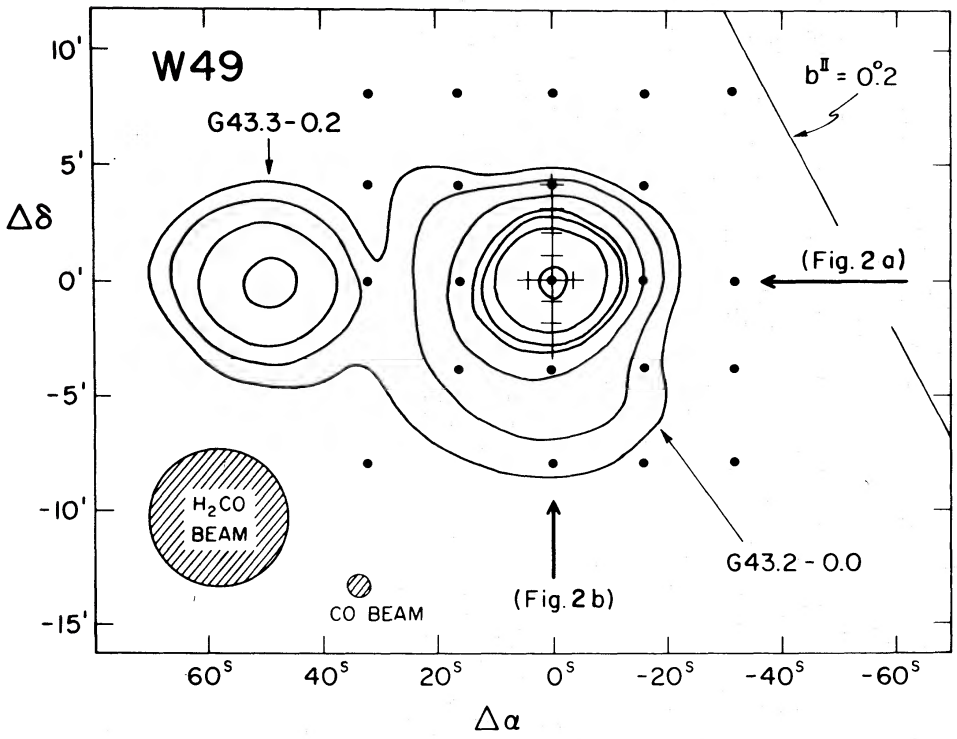

FIG. 1*a*

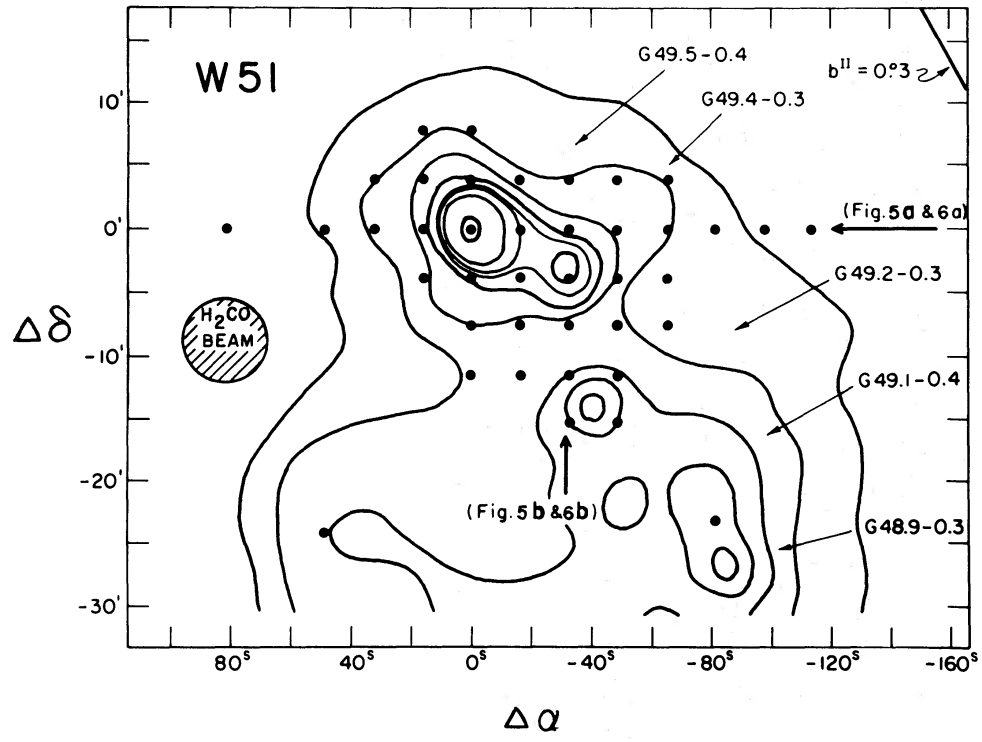

FIG. 1*b*

FIGS. 1*a* and 1*b*.—Locations of H_2CO and CO observations in W49 (1*a*) and W51 (1*b*) are indicated by dots and crosses superposed on isophotes of 6-cm continuum radiation (Goss and Shaver 1970; HPBW = 4′). The orientations of the spatial-velocity contour diagrams (figs. 2, 5, and 6) and the H_2CO and CO beams are also shown. Isophote levels are at 1°, 2°, 4°, 8°, 12°, 16°, and 60° K (T_A).

TABLE 1

PARAMETERS OF H II REGIONS AND MOLECULAR VELOCITIES IN W49 AND W51

Source (1)	G-Component (2)	$V_{H109\alpha}$ [km s^{-1}] (3)	D [kpc] (4)	$2R_{H\,II}$ [pc] (5)	$\langle N_e \rangle$ [10^2 cm^{-3}] (6)	$M_{H\,II}$ [$10^3\ M_\odot$] (7)	V_{OH} (absorption) [km s^{-1}] (8)	V_{OH} (emission) [km s^{-1}] (9)	V_{H_2O} [km s^{-1}] (10)	V_{H_2CO} [km s^{-1}] (11)	V_{CO} [km s^{-1}] (12)
W49....	43.2–0.0	+ 8.9	14.1	18.7	1.8	~5.0	...	+ 3 (8)	− 4 (5)	...	+ 3 (9)
							+17 (5)	+15 (10)	+10 (8)	+11 (15)	+12 (7)
							...	...	+39	+39	...
							...	...	+60 (5)	+62	...
W51....	49.5–0.4	+58.2	7.3	9.4	3.7	3.7	+50?	...	...	...*	?
							...	+58 (4)	+60 (8)	...*	+57 (17)
							+63 (7)	...	...	+65 (9)	+65 (4)†
	49.4–0.3	+52.8	8.5	12.7	1.6	4.0	...	...	...	+50 (4)	+51 (6)
							...	...	...	+64 (7)	+65 (7)
	49.2–0.3	+67.2	6.6	3.7	4.7	0.3	...	...	...	+65 (4)	...
	49.0–0.3	+63.2	6.6	11.6	1.2	2.2	...	...	...	+66 (4)	+66 (8)

* Blended with the 65 km s^{-1} line.

† Self-absorption feature (see § II*b*[i]).

NOTE.—Parameters of the H II regions are from Gordon and Wallace (1971); Mezger *et al.* (1967); Reifenstein *et al.* (1970); Schraml and Mezger (1969); Wilson *et al.* (1970); and Wynn-Williams (1969). Velocities of OH (Weaver *et al.* 1968) and H_2O (Buhl *et al.* 1969) are included when similar to H_2CO and CO lines observed here. Broad molecular lines ($\Delta V \gtrsim 4$ km s^{-1}) are listed by their central velocities and width, in parentheses.

with the linear feed. The NRAO 384-channel autocorrelation receiver was used in the total power mode with a bandwidth of 2.5 MHz (~ 155 km s^{-1} at 6 cm), and the data were cosine filtered to a velocity resolution of 0.81 km s^{-1}. (Higher spectral resolution is unwarranted in studies of cloud structure because of the H_2CO hyperfine-structure width of ~ 0.5 km s^{-1}. In a few positions where low continuum intensities necessitated integrations up to an hour, the receiver was frequency switched at 1 Hz between the signal band and two adjacent reference bands. Radial velocities of the observed lines were computed using standard components for solar motion relative to the local standard of rest (LSR, Allen 1963), and 4829.65961 MHz as the rest frequency of the H_2CO 1_{11}–1_{10} rotation transition (Tucker, Tomasevich, and Thaddeus 1970).

Observations of the 6-cm H_2CO line, to date, indicate that it is reasonable to adopt a constant excitation temperature. The 6-cm transition has been seen only in absorption, in front of a wide variety of continuum sources as well as in dark nebulae behind which there is no discrete source of continuum radiation (Palmer *et al.* 1969). Thus the excitation temperature of the 6-cm levels, T_{12}, is very low in almost all molecular clouds. An estimate of the excitation temperature from the hyperfine intensity ratio in dark nebulae (Heiles 1972), where the absorption line is observed against the 2.7° K cosmic background radiation, gives $T_{12} = 1.7°$ K; and because there is no strong observational evidence that T_{12} varies, we assume in calculating the 6-cm optical depth τ that T_{12} is constant and equal to 1.75° K. (Small deviations, in the range $1° \text{ K} < T_{12} < 3°$ K, will not substantially effect the derived parameters.) For a plane-parallel cloud of formaldehyde molecules which uniformly covers all radiation sources contained in the antenna beam, the radiative-transfer relation is

$$T'_L = (T'_c + T'_{\text{bg}} - T_{12})(1 - e^{-\tau}), \tag{1}$$

where T'_L, T'_c, and T_{bg} are the brightness temperatures of the line, the discrete sources, and the cosmic background, and τ is the optical depth. (Absorption lines correspond to positive values of T'_L and emission to negative values.)

Although the above is valid for the assumed conditions, in practice equation (1) serves only as a definition of apparent optical depth rather than true optical depth, which will be greater, since molecular clouds may be nonuniform or, as is frequently the case, be situated behind the most intense sources. However, where the same cloud is observed at several positions, with different continuum intensities T'_c, equation (1) may be used to determine how various geometrical arrangements of the continuum sources and a uniform cloud of absorbing molecules (for which the *true* optical depth is a constant) would appear observationally. We assume that both T_{12} and T'_{bg} are much less than T'_c, as is often the case for the 6-cm H_2CO lines. If this uniform cloud is in *front* of the continuum sources, the absorption line temperature T'_L will vary in *direct* proportion to the continuum intensity at each position while the apparent optical depth τ, determined by equation (1), will be constant across the cloud. On the other hand, if the cloud is *behind* the continuum sources, the absorption line temperature will remain constant, and the apparent optical depth will vary *inversely* with the continuum intensity. Assuming reasonable uniformity in the structure and excitation temperature, these considerations can be used to determine the relative positioning along the line of sight of the cloud and the sources.

The gas column densities corresponding to a given formaldehyde line may be calculated from its integrated optical depth. If $\tau \ll 1$ and the equivalent width W [km s^{-1}] is defined by

$$W = \int_{\text{line}} [1 - e^{-\tau(v)}] dv, \tag{2}$$

then the column density N_1 [cm^{-2}] of H_2CO molecules in the lower 6-cm level is

$$N_1 = 2.90 \times 10^{12} W/[1 - \exp(-0.23/T_{12})] . \quad (3)$$

The total formaldehyde column density is $3N_1 \rightarrow 7N_1$ if the populations of the other rotational levels are described by Boltzmann distributions at 3°–20° K.

The column density of hydrogen (atomic and molecular), $N_{\Sigma H}$, is apparently also proportional to the equivalent width of the H_2CO line. Observations of local dark nebulae suggest that a cloud with about 5 mag of visual extinction will have a 6-cm equivalent width of ~ 1 km s^{-1} (Kutner *et al.* 1973); then taking a gas-to-dust ratio of $\simeq 2 \times 10^{21}$ H/magnitude, we obtain the approximate relation,

$$N_{\Sigma H} = W \times 10^{22} \text{ cm}^{-2} . \quad (4)$$

The validity of equation (4) rests on a constant formaldehyde-to-dust ratio in all dense clouds and a constant hydrogen-to-dust ratio in regions of both atomic and molecular hydrogen. Equation (4) is equivalent to $N_1/N_{\Sigma H} = 2.5 \times 10^{-9}$.

b) CO and CS

The millimeter-wavelength lines of CO and CS in W49 and W51 were observed with a front-end receiver built at Bell Telephone Laboratories in Holmdel, New Jersey, and the NRAO 36-foot antenna at Kitt Peak, Arizona. The beam efficiency (η) and width (HPBW) for the telescope are approximately 0.6 and 1′ at the CO and CS frequencies. Noise calibration was provided by a synchronous chopper wheel which alternately viewed the sky and a room-temperature absorbing sheet. These antenna temperatures (T_A) can be converted to brightness temperatures (T_B) by the following relation:

$$\frac{1}{[\exp(h\nu/\kappa T_B) - 1]} = \frac{\kappa T_A}{\eta h\nu} + \frac{1}{[\exp(h\nu/\kappa T_{bg}) - 1]} . \quad (5a)$$

For $h\nu/\kappa$ and $T_{bg} < T_B$ (i.e., $T_B > 10°$ K), this simplifies to

$$T_B \simeq T_A/\eta . \quad (5b)$$

Interpretation of the CO and CS lines is complicated by obvious variations in the excitation temperatures of these transitions from cloud to cloud and even within single clouds. All of the 2.6-mm CO lines reported here are optically thick, and the different intensities must thus reflect the excitation temperature T_{01} of the $J = 0, 1$ levels (assuming that the clouds are not patchy; see eq. [1]). The spontaneous transition rate A_{10} is 6×10^{-8} s^{-1}, and the rotational excitation cross-section of CO for *neutral* collisions is $\sim 10^{-15}$ cm^2. A neutral-hydrogen density n greater than 10^3 cm^{-3} will therefore be sufficient to couple the 2.6-mm transition to the gas kinetic temperature, and the CO brightness temperature in dense clouds will give a reasonable estimate of the kinetic temperature. (The collisional excitation rate by *electrons* will exceed that by neutrals if the fractional electron abundance is $\geq 3 \times 10^{-3}$, which is definitely not expected in most dense molecular clouds [Solomon and Werner 1971].) Variations in T_{01} will then be caused primarily by changes in either the gas density (if $n < 10^3$ cm^{-3}) or the gas kinetic temperature (if $n > 10^3$ cm^{-3}); an increase in T_{01} (or the line intensity) may indicate not only a hotter region of gas but also perhaps a denser region. Similar arguments can be made for the CS transitions (Penzias *et al.* 1971*b*). The relatively large values of A_{32} and A_{21} (6.5×10^{-5} and 2.1×10^{-5} s^{-1}) suggest that these levels will not couple to the gas unless $n \geq 10^6$ cm^{-3}. These lines have therefore been taken as indicators of high-density regions; however, alternative possibilities are suggested in § IV.

In order to estimate the optical depth of the CO line and as part of a program on isotope ratios (see Penzias *et al.* 1972*a*) we observed the ^{13}CO and $C^{18}O$ lines in W51 and the ^{13}CO lines in W49. As can be seen from figure 9*a*, the intensity ratio $T_{^{13}CO}/T_{C^{18}O} = 7 \pm 1.1$ in W51, which is very close to the predicted ratio of 5.5, assuming terrestrial abundances $[^{12}C/^{13}C] = 89$ and $[^{16}O/^{18}O] = 499$. We regard this as substantial evidence in favor of terrestrial isotope ratios for both carbon and oxygen in W51 and assume that the same holds for W49.

The optical depth τ_{01} of the CO line can then be estimated from

$$\tau_{01} = 89 \ln \left(\frac{1}{1 - T_{^{13}CO}/T_{CO}} \right) . \tag{6}$$

The above assumes that the excitation temperature is the same for all isotopic species and may introduce some error since the thick CO lines originate from the closest optical depth at each velocity whereas the optically thin isotope lines have contributions through the cloud.

If all CO rotational levels are in thermal equilibrium at T_{01}, the column density of CO, N_{CO}, is given by

$$N_{CO} = \frac{2.85 \times 10^{14} \tau_{01} \Delta V T_{01}}{[1 - \exp(-5.5/T_{01})]} \text{ cm}^{-2} , \tag{7}$$

where ΔV is the line width in km s^{-1}. A *lower limit* to the total hydrogen column density is obtained by assuming that all the carbon is bound up in carbon monoxide. A C/H abundance ratio of 3×10^{-4} (Allen 1963) then implies that

$$N_{\Sigma H} \geq 3.3 \times 10^{3} N_{CO} \text{ cm}^{-2} . \tag{8}$$

III. RESULTS

The H_2CO observations for W49 and W51 are presented in both velocity-spatial and two-dimensional spatial contour diagrams. The spatial coordinates used in these diagrams are centered on the strongest continuum radiation peak in each region (Reifenstein *et al.* 1970):

$$\text{W49A(G43.2}-\text{0.0)}: \quad \alpha_{1950} = 19^{h}07^{m}54^{s}; \ \delta_{1950} = 9°01'01'' .$$

$$\text{W51 (G49.5}-\text{0.4)}: \quad \alpha_{1950} = 19^{h}21^{m}23^{s}; \ \delta_{1950} = 14°24'29'' .$$

In addition to the figures, line measurements (generally at positions of maximum apparent optical depth) are listed in table 2. The contents of the columns in table 2 are as follows: column (1), cloud name; columns (2) and (3), coordinate displacements at which greatest optical depth was observed; column (4), radial velocity at maximum optical depth; column (5), full line width at half-intensity; column (6), antenna temperature of 6-cm H_2CO absorption line at this position; column (7), peak optical depth calculated using equation (1); column (8), equivalent width from equation (2); column (9), column density of formaldehyde molecules in the 1_{11} rotational level, N_1, as calculated from equation (3); column (10), estimated angular extent of the cloud; column (11), physical diameter calculated assuming the cloud is located near W49 (14.1 kpc) or W51 (6.5 kpc); column (12), maximum 2.6-mm CO antenna temperature in the cloud (these lines were not necessarily observed at the position of maximum H_2CO optical depth given in cols. [2] and [3]); column (13), typical column density of hydrogen $N_{\Sigma H}$, estimated in § III from the H_2CO and CO lines (as discussed in § III, these estimates are probably minima); column (14), mass of molecular cloud.

TABLE 2

RESULTS FOR W49 AND W51 MOLECULAR CLOUDS

Cloud and Line Velocity [km s^{-1}] (1)	$\Delta\alpha$ [s] (2)	$\Delta\delta$ [′] (3)	v_{LSR} [km s^{-1}] (4)	Δv [km s^{-1}] (5)	T_L [° K] (6)	τ (7)	W [km s^{-1}] (8)	N_1 [10^{13} cm^{-2}] (9)	$\Delta\theta$ [′] (10)	$2R$ [pc] (11)	T_{CO} [°K] (12)	$\bar{N}_{\Sigma H}$ [10^{21} cm^{-2}] (13)	M_{cloud} [10^4 $M_\odot$] (14)
W49:													
3*.....	0	0	3.0	...	0.23	0.019	...	...	(6)	(24)	3.8	$\gtrsim$7	>2
14.....	−16	+5	14.2	15	0.28	0.21	2.1	4.9	9	37	5.2	10	10
39.....	0	0	39.2	$\lesssim$3	0.62	0.051[2]	0.12	0.28	>12	...	...†	1	...
62.....	0	0	62.4	$\lesssim$3	0.72	0.060[2]	0.16	0.37	>12	...	...†	1	...
W51:													
50.....	−48	0	48.3	4	0.23	0.095	0.21	0.49	(15)	(28)	8.0	2	...
50‡.....	−24	−2	50.5	6	0.41	0.68	4.0	9.3	10	19	8.0	40	...
57.....	+20	−4	58.8	7	0.55	0.094	0.64	1.5	(10)	(19)	15.4	60	10
65.....	−24	−2	63.4	5	1.90	0.31	1.7	3.9	>10	>19	8.4	10	6

* In 6-cm H_2CO spectra, this feature was never distinct from the low-velocity wing of the 14 km s^{-1} line.

[2] This value was obtained in the least squares determination of T_{12} from all observations of this line (see § III*a*[ii]).

† Velocity resolution of the W49 CO observations was ~4 km s^{-1}.

‡ The measurements in this line of the table assume that the cloud is absorbing only the cosmic background radiation, i.e., $T_c' = 0°$ K in equation (1) (see § III*b*[ii]).

NOTE.—Columns (2)–(11) refer exclusively to H_2CO observations; the estimates in columns (13) and (14), obtained from both the CO and H_2CO observations, should in most cases be taken as minima (see § III). All the 6-cm H_2CO measurements are at the position of maximum apparent optical depth except the second set of measurements for the W51 50 km s^{-1} cloud (see ‡ above). Particularly uncertain values are enclosed in parentheses.

TABLE 3

CO OBSERVATIONAL RESULTS FOR W49A

POSITION RELATIVE TO W49A		LINE 1 (3 ± 2 km s^{-1}):	LINE 2 (12 ± 2 km s^{-1}):
$\Delta\alpha$[s] (1)	$\Delta\delta$[′] (2)	T_{CO}[°K]* (3)	T_{CO}[°K]* (4)
0	+4	< 0.2	1.4
0	+3	< 0.3	3.0
0	+2	≤1.3†	4.5
0	+1	2.5	3.8
0	0	3.8	5.2
0	−1	< 0.6	2.3
0	−2	< 0.3	1.4
0	−3	< 0.4	1.1
4	0	2.4	3.9
−4	0	2.5	3.7

* Because the velocity resolution was only 4 km s^{-1}, the line antenna temperatures listed in columns (3) and (4) are probably underestimated.

† The wing of line 2 extends smoothly out to −5 km s^{-1}.

Parameters of the CO emission lines near W49A, including the displacement coordinates, the peak antenna temperatures, and radial velocities of the two observed features, are listed in table 3. The CS observations are presented and discussed in § IV.

a) W49

Figures 2*a* and *b* are contour diagrams of H_2CO line temperature plotted in coordinate-velocity planes. They show observations along east-west and north-south strips which cross the W49A peak (see fig. 1*a*).

The 6-cm H_2CO spectrum in W49A has lines at 14, 39, and 62 km s^{-1}. The intensity variations are proportional to the continuum intensities at each position, indicating that they all originate in front of W49A. The CO spectrum shows an additional feature at 3 km s^{-1}. The 3 and 14 km s^{-1} clouds may be near the H II regions since the H109α recombination line is observed at 8.9 km s^{-1}, while the two higher-velocity H_2CO lines probably originate in clouds very distant from the H II region.

i) *Gas at 3 and 14* km s^{-1}

Both the 3 and 12 km s^{-1} CO lines in W49 (table 3 and fig. 3) are strongest at the continuum peak and maintain constant (± 2 km s^{-1}) velocities across the source. (We group the 12 km s^{-1} CO and the 14 km s^{-1} H_2CO lines together because their widths are much larger than the 2 km s^{-1} peak velocity difference.) The half-intensity contours for the two CO lines have diameters of 2.5 and 4′, respectively (as compared to the half-power width of 3.′1 for W49A [Mezger and Henderson 1967]), and the centers of these contours are ~1′ north of W49A. This good agreement in size, position, and velocity of the two CO emission features with the H II region indicates a close physical relationship.

The intensity falloff, away from the H II region, of the 12 km s^{-1} CO line could be due to a decrease of (1) the CO optical depth, (2) the density of exciting particles (neutrals and electrons), or (3) the gas kinetic temperature. As can be seen from the H_2CO results in figure 4, the cloud is much larger than the H II region and not concentric. The maximum equivalent width is observed 6′ northwest of the H II region, and the full extent of the cloud has not been mapped. It may extend 12′ to the east of W49A since Whiteoak and Gardner (1970) observe a 6-cm line at 16.6 km s^{-1} in the

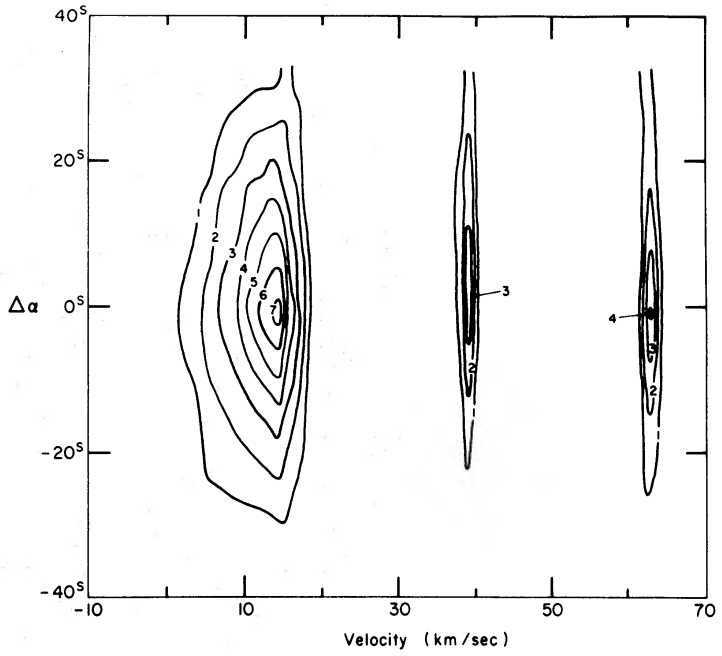

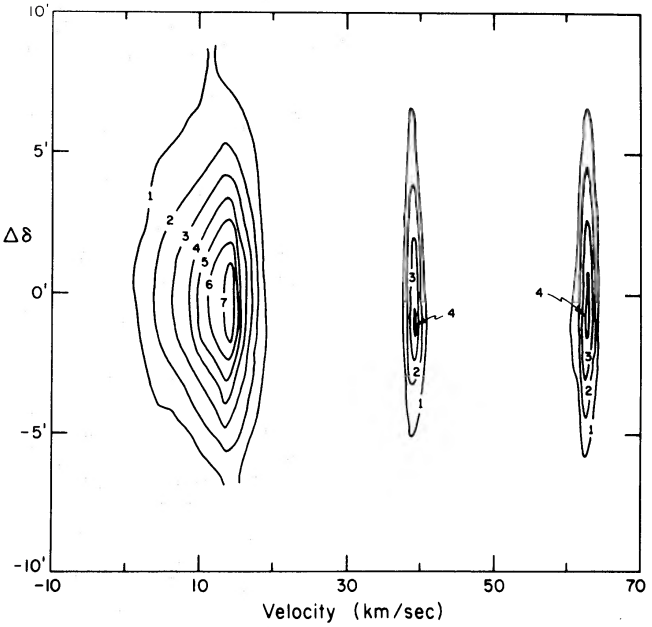

FIG. 2*a* (*top*).—Contour diagram of 6-cm H_2CO absorption $T_L(v)$, in the ($\Delta\alpha$, velocity)-plane at $\Delta\delta = 0'$. Spatial orientation of diagram is shown in fig. 1*a*; $\Delta\alpha$ and $\Delta\delta$ are right ascension and declination displacements from the W49A continuum peak. Contour unit is 0.15° K in antenna temperature.

FIG. 2*b* (*bottom*).—Contour diagram of 6-cm H_2CO absorption $T_L(v)$ in the ($\Delta\delta$, velocity)-plane at $\Delta\alpha = 0^s$. $\Delta\alpha$, $\Delta\delta$, and contour levels are defined as in fig. 2*a*.

direction of W49B. The *increasing* H_2CO column density to the northwest of W49A suggests strongly that the first and second (if the path length does not increase in the northwest of the cloud) of the above explanations are unlikely. In this cloud we therefore have evidence, albeit not conclusive, of highest kinetic temperatures close to the H II region. It is noteworthy that the CO line temperature 4′ north of W49A is similar to that observed in many dark nebulae by Penzias *et al.* (1972*b*); perhaps the high temperatures near the H II region are caused by heating of the cloud by the H II region. At any rate, we may safely conclude that the CO *excitation* temperature is highest near the H II region and that consequently the sizes of molecular regions are not reliably determined from intensity variations of a single molecular emission line (e.g., CO).

Figure 4 indicates a size of 9 × 9′ and average equivalent width of unity in the H_2CO line at 14 km s^{-1}. This yields a mass $\sim 10^5\ M_\odot$ (using eq. [4]), which is similar to that of molecular clouds in the galactic center and over 10 times that of the associated H II region (table 1). The CO observations yield estimates of the hydrogen column density which are consistent with those ($\sim 10^{22}$ cm^{-2}) obtained from the H_2CO lines. If the $^{12}C/^{13}C$ abundance ratio is terrestrial and the other assumptions outlined in § II*b* are valid, the optical depths of the ^{13}CO and CO lines shown in figures 3 are 0.7 and 60. Using equations (7) and (8), we find CO and hydrogen column densities of 2×10^{18} cm^{-2} and $\gtrsim 7 \times 10^{21}$ cm^{-2} in both the 3 and 12 km s^{-1} clouds. The average gas densities in the molecular clouds are also within a factor 2 of the electron density (~ 200 cm^{-3}) in the extended component of the H II region.

The velocity characteristics of the 14 km s^{-1} H_2CO line are complicated, but there is a slight velocity gradient across the face of the cloud in a direction perpendicular to the galactic plane (fig. 4). In further support of the idea that this cloud is near W49A, we note that Gordon and Wallace (1971) observe a similar gradient for the H109α recombination line of W49A. Two possible explanations of the gradient are rotation about an axis parallel to the galactic plane and expansion or contraction of the cloud along the direction of the gradient. Gordon and Wallace attribute the recombination-

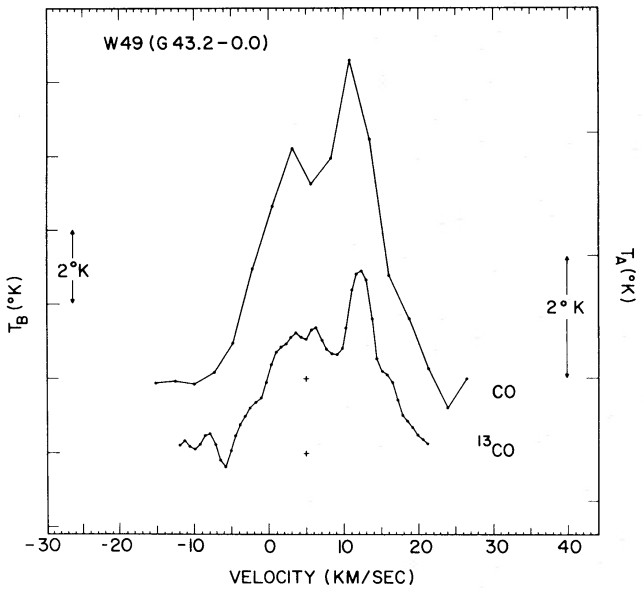

FIG. 3.—Spectra of CO and ^{13}CO emission at the W49A continuum peak ($\Delta\alpha = 0^s$, $\Delta\delta = 0'$). The vertical scale on the right is antenna temperature T_A, and that on the left is T_A/η ($\approx$ brightness temperature T_B, for $T_B > 10°$ K).

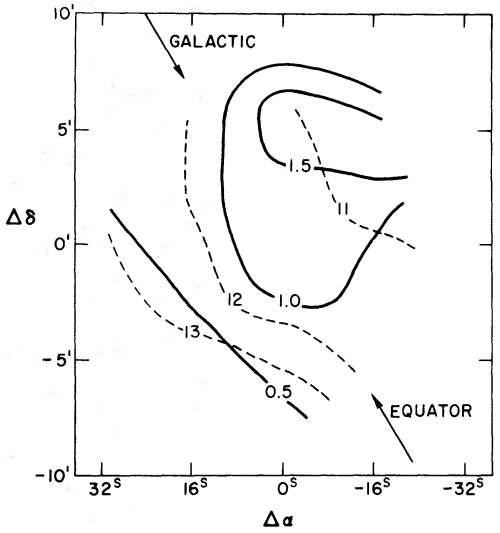

FIG. 4.—Contour diagram of equivalent width (*solid contours*) and mean velocity (*dashed contours*) in $(\Delta\alpha, \Delta\delta)$-plane for the 14 km s^{-1} H_2CO line in W49A. Units of W are km s^{-1}.

line gradient to expansion of hot gas at the ionization front against the surrounding anisotropic, cold H I gas. However, it seems unlikely that the gradient can be explained by a phenomenon as localized as the ionization front since the H_2CO lines, which clearly refer to a much larger volume than the H II region, show the same effect.

As we have described above, the CO and H_2CO observations furnish strong evidence for the 14 km s^{-1} molecular cloud being very near to W49A, although its radial velocity is about 5 km s^{-1} greater than the H II region. Moreover, the intensity variations of the H_2CO line indicate that the cloud is situated in front of W49A; this molecular cloud is therefore moving towards the H II region at 5 km s^{-1}. The absence of a distinct H_2CO counterpart to the 3 km s^{-1} CO cloud (at a limit of one-seventh the optical depth of the 14 km s^{-1} H_2CO line), together with the relatively slow variation of the absorption temperatures across W49A at 3 km s^{-1}, suggests that this gas may be behind the H II region and thus is also approaching the H II region at about 6 km s^{-1}. Indeed, the shape of the 14 km s^{-1} H_2CO line is similar to that expected from a spherical shell collapsing on the H II region at a velocity of 5 km s^{-1}. But we must caution against such a simple picture, since the two CO lines show no indication of velocity shifts near the edge of the H II region. Moreover, the apparent optical depths at intermediate velocities of 5–10 km s^{-1} in the H_2CO line are constant across W49A within the noise limit of these observations. Thus the fading of the extended low-velocity wing of the 14 km s^{-1} line as one moves off the H II region (fig. 2) appears to be not a real change in the velocity distribution of the molecules but merely the effect of decreasing illumination in the profile by the lower continuum intensities. (This point definitely requires further investigation with a smaller telescope beam and higher sensitivity.)

ii) *Gas at 39 and 62* km s^{-1}

The narrow H_2CO lines at 39 and 62 km s^{-1} may originate from dark clouds that happen to be along the line of sight to W49A. Carbon monoxide emission was not detected at these velocities, but this was probably because of the low velocity resolution ($\sim$4 km s^{-1}) of the CO observations. We have used the H_2CO lines to estimate the excitation temperature of the 6-cm levels from the observed variations in line temperature as a function of the continuum intensity. A least-squares solution was found

using equation (1) and assuming that the peak optical depth and T_{12} were constant in each of the clouds at all positions for which the lines were visible above the noise. The combination of the separate T_{12} calculated for each cloud yields $T_{12} = 1.76° \text{ K} \pm 1.2° \text{ K}$, consistent with the value obtained for dark clouds in the solar neighborhood (§ II*a*). These two lines would be difficult to observe in absorption against only the microwave background, because their optical depths (~ 0.055) would produce a line of less than 0.05° K if the excitation temperature has the above value. The small equivalent widths of the lines are suggestive of low gas densities in the two clouds.

Of great potential interest is the fact that H_2O emission lines are also observed at 39 and 60 km s^{-1} in W49A (see fig. 2 of Buhl *et al.* 1969). Although it cannot be ruled out, a coincidental velocity correspondence between H_2O and H_2CO features seems unlikely in view of the number of lines in each spectrum. This raises the interesting possibility that some of the H_2O sources are located in foreground dark clouds which are not intimately connected with the H II regions. Additional searches for narrow H_2CO lines at the velocities of H_2O lines must be carried out in order to check this possibility.

b) W51

Figures 5 and 6 are contour diagrams of line temperature and optical depth, respectively, for H_2CO absorption in W51. The spatial orientation of the two sets of data is shown in figure 1*b*.

In discussing the molecular lines of the W51 region, we consider three separate clouds with velocities of 50, 57, and 65 km s^{-1}. Our observations indicate that all three clouds are in the vicinity of the W51 thermal sources and thus may be physically related; but because their lines and spatial characteristics are very different, we will discuss them separately.

i) *Gas at 65* km s^{-1}

The most intense 6-cm absorption line in W51 has a velocity of ~ 65 km s^{-1}. Its maximum antenna temperature of 4.5° K in the direction of G49.5−0.4 implies that the 65 km s^{-1} cloud lies in front of this H II region, and increases in the line temperature near the sources G49.4−0.3 and G49.2−0.3 suggest that it is also in front of them (see fig. 5*b*). Contours of equivalent width and mean velocity for this line are presented in figure 7.[2] The line has a maximum equivalent width of 2.01 km s^{-1} 4′ north of G49.5−0.4 while the angular diameter of G49.5−0.4 is only 4′.3. (Mezger and Henderson 1967), indicating that the molecular column density definitely does not peak near the center of this intense source. In fact, comparison of the continuum and equivalent width maps (figs. 1*b* and 7) shows that the molecular cloud extends over much of the W51 region with its shape elongated along the direction in which the thermal sources lie (i.e., parallel to the galactic plane)!

Wilson *et al.* (1970) and Reifenstein *et al.* (1970) have detected H109α recombination lines from seven of the thermal sources in W51, five of which are shown in figure 1*b*. The two northernmost sources, G49.5−0.4 and G49.4−0.3, have velocities of 58.2 and 52.8 km s^{-1} whereas the more southerly sources shown in figure 1*b* have an average velocity of 67.7 km s^{-1}. On the basis of this velocity difference between the southern and northern sources, Wilson *et al.* conclude that there are two distinct and unrelated associations of giant H II regions ($\sim 3 \times 10^3 M_\odot$) at distances of 6.5 and 8.0 kpc. However, as can be seen from figure 7, the distribution of the 65 km s^{-1}

[2] In calculating W, the integration was between 55 and 70 km s^{-1}; a small contribution from the 57 km s^{-1} cloud is therefore included. The absence of contours in the lower left portion of the figure should not be taken as indicating that the line is undetectable, since no observations were made there.

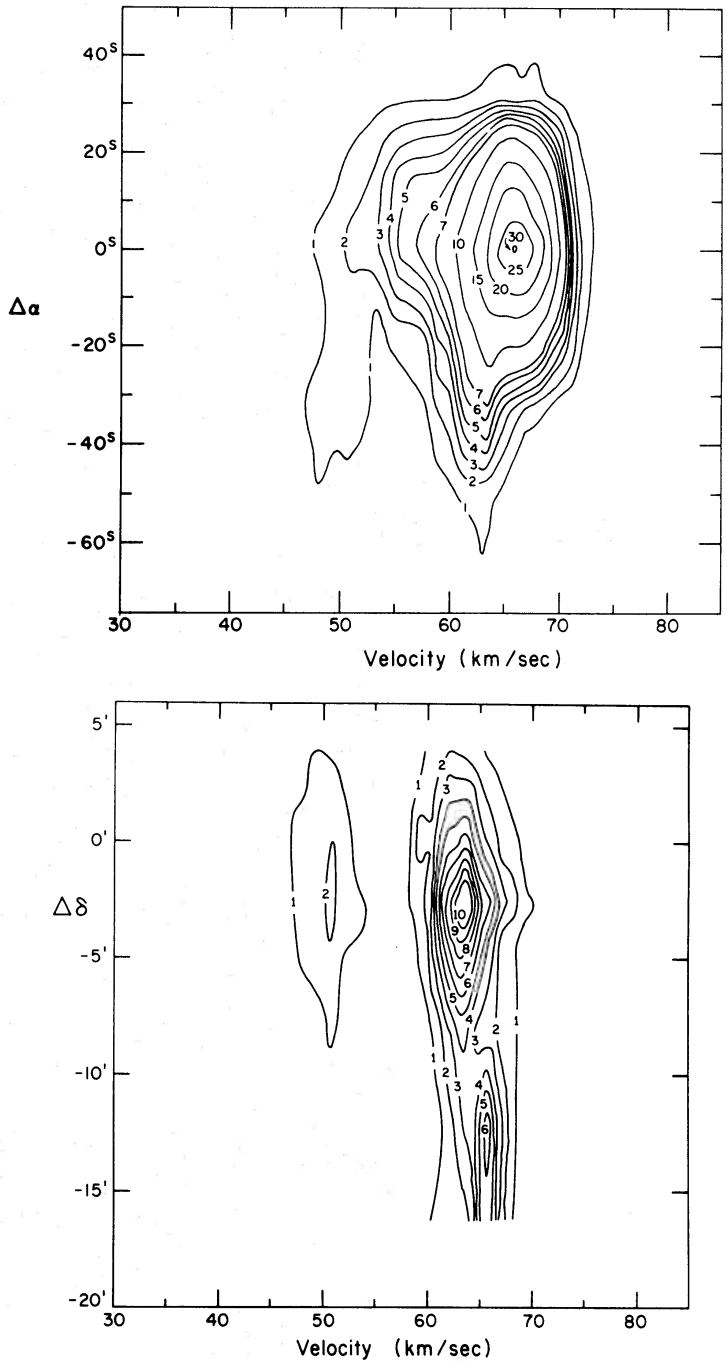

FIG. 5*a* (*top*).—Contour diagram of 6-cm H_2CO absorption $T_L(v)$, in the ($\Delta\alpha$, velocity)-plane at $\Delta\delta = 0'$. Spatial orientation of diagram is shown in fig. 1*b*; $\Delta\alpha$ and $\Delta\delta$ are right ascension and declination displacements from W51 (G49.5 − 0.4). Contour unit is 0.15° K in antenna temperature.

FIG. 5*b* (*bottom*).—Contour diagram of 6-cm H_2CO absorption $T_L(v)$ in the ($\Delta\delta$, velocity)-plane at $\Delta\alpha = -32^s$. $\Delta\alpha$, $\Delta\delta$, and contour levels are defined as in fig. 5*a*.

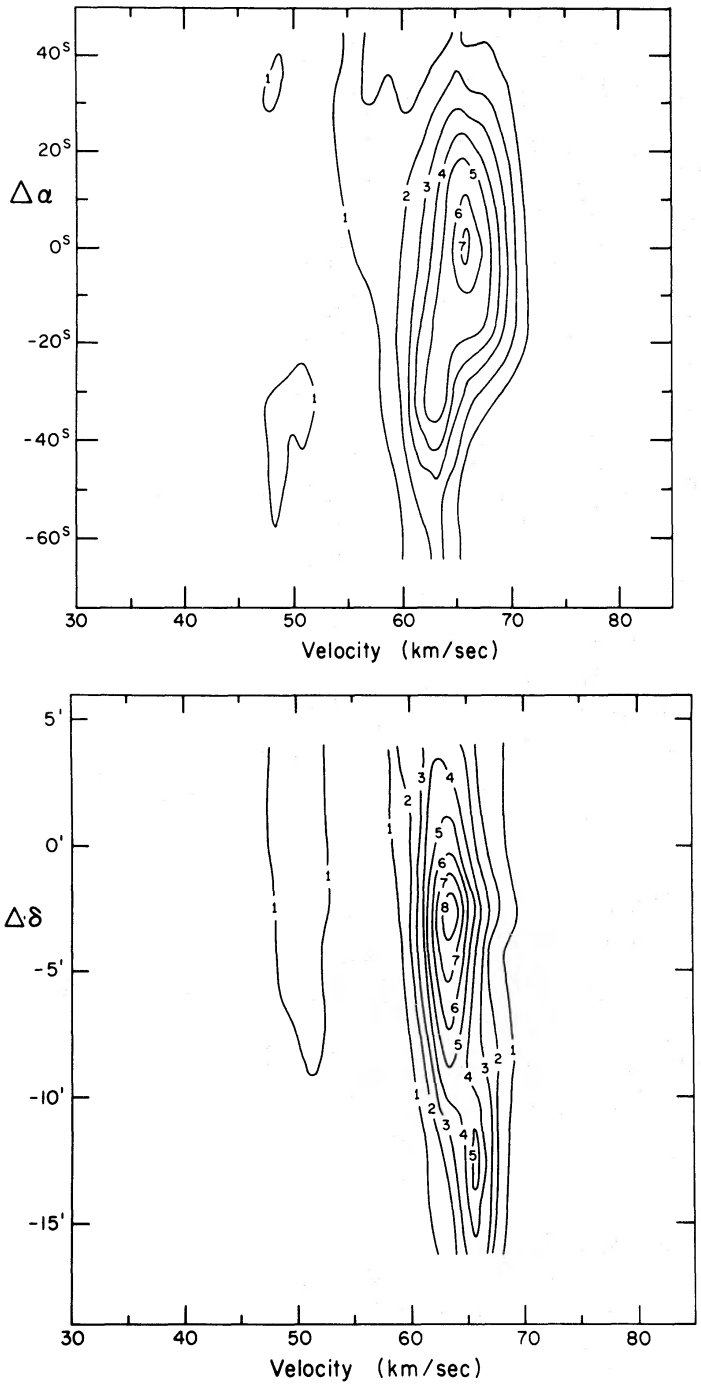

FIG. 6*a* (*top*).—Contour diagram of H_2CO optical depth $\tau(v)$, in the ($\Delta\alpha$, velocity)-plane at $\Delta\delta = 0'$. Optical-depth unit is 0.03. (Optical depths in fig. 6 were calculated from data of fig. 5, the measured continuum temperatures, and eq. [1].)

FIG. 6*b* (*bottom*).—Contour diagram of H_2CO optical depth $\tau(v)$ in the ($\Delta\delta$, velocity)-plane at $\Delta\alpha = -32^s$. Optical-depth unit is 0.03.

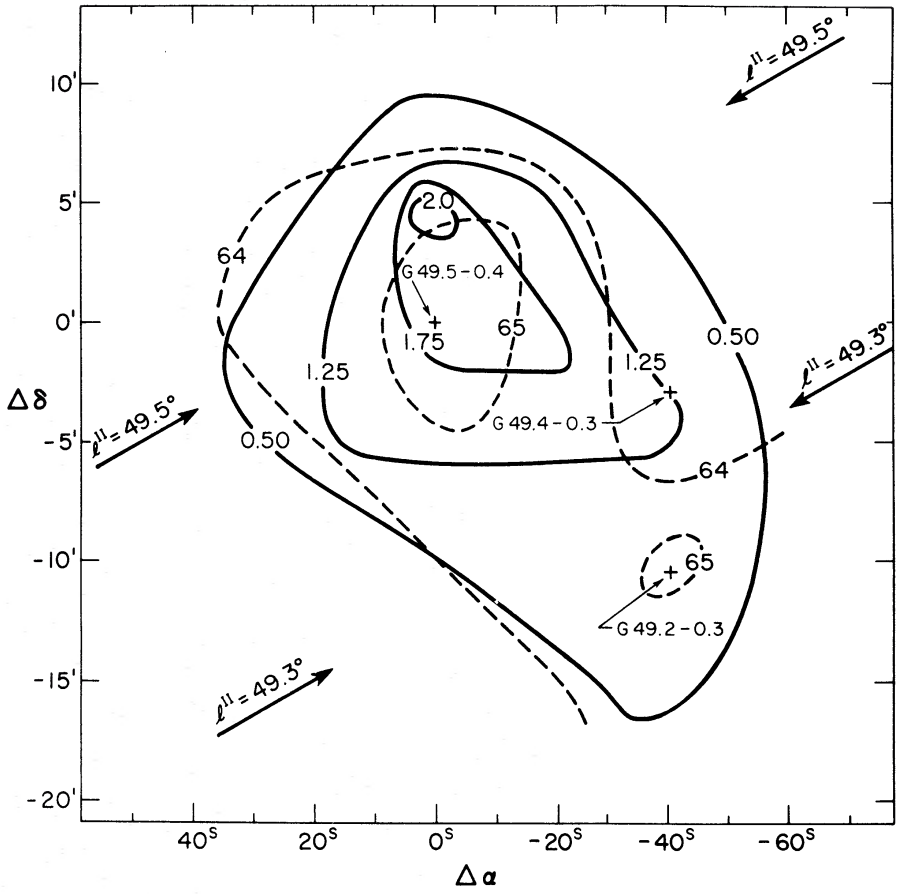

FIG. 7.—Contour diagram of equivalent width (*solid contours*) and mean velocity (*dashed contours*) in $(\Delta\alpha, \Delta\delta)$-plane for the 65 km s^{-1} H_2CO line in W51. $\Delta\alpha$ and $\Delta\delta$ are defined as in fig. 5*a*, and units of W are km s^{-1}.

molecules more closely resembles that of all the thermal sources rather than just the southerly ones. The cloud is probably not associated with one single H II region but instead is part of one large complex that includes both molecular clouds and H II regions. This would in turn imply that all the H II regions are at nearly the same distance. There is a definite shifting of the 65 km s^{-1} line peak to higher velocities in the vicinity of the higher-velocity southern sources (fig. 6*b*) and a weak suggestion that the mean velocity of the gas (fig. 7) is $\sim$1 km s^{-1} higher in the direction of the two sources G49.5−0.4 and G49.2−0.3. We also note that the highest optical depths in figures 6*a* and 6*b* occur at the right ascension of G49.5−0.4 and the declinations of G49.4−0.3 and G49.2−0.3. Although possibly real, these local increases in peak optical depth near the H II regions could also arise from underestimation of the continuum intensity near the continuum peaks or too low a value for T_{12} in equation (1). High-resolution, low-noise observations are certainly required before the effect can be considered real.

From the 6-cm data in figure 7 and assuming that the cloud is near the H II regions, we find that its mass is $6 \times 10^4\ M_\odot$—almost 10 times the mass of the three W51 H II regions contained in this same portion of sky (table 1). The average hydrogen column density ($\sim 10^{22}$ cm^{-2}) corresponds to a gas density of $\sim$200 cm^{-3}.

The CO spectrum of G49.5−0.4 (fig. 9*a*) shows a strong, broad line at 57 km s^{-1} and a secondary peak at 69 km s^{-1}. At 65 km s^{-1} where the peak H_2CO absorption occurs, there is only a local minimum in the CO emission. In contrast, the CO spectrum of G49.0−0.3 (fig. 9*b*) shows a single peak at 66 km s^{-1}. The 69 km s^{-1} emission, which at first would appear to be a counterpart of the 65 km s^{-1} H_2CO absorption, is observed only where the 57 km s^{-1} line is intense and thus is probably not from a separate cloud. We suggest that this emission is merely the wing of the 57 km s^{-1} line and that the local minimum is due to absorption by cold CO in the large 65 km s^{-1} cloud lying in front of the 57 km s^{-1} emission region. This interpretation is supported by the ^{13}CO and $C^{18}O$ spectra of figure 9*a* which show no peak at 69 km s^{-1} but instead a shoulder at about 65 km s^{-1}. The CO self-absorption implies an excitation temperature T_{01}, probably also a kinetic temperature (§ II*b*), of only $\sim 9°$ K (using eq. [5a]) in the 65 km s^{-1} cloud near G49.5−0.4. In the direction of G49.9−0.3 (fig. 9*b*), T_{01} is much higher ($\sim 16°$ K) and the CO/^{13}CO intensity ratio of 5 gives $\tau_{01} = 20$. The CO column density is then $\sim 10^{18}$ cm^{-2}. Near G49.5−0.4 the observed CO/^{13}CO intensity ratio of 1.5 at 65 km s^{-1} could imply that $\tau_{01} \sim 100$; however, this is certainly an overestimate, since, based on our interpretation above, the 65 km s^{-1} ^{13}CO emission, if optically thin, will contain a contribution from gas in the hot 57 km s^{-1} cloud whereas the optically thick CO emission will come solely from the cold H_2CO cloud. A reliable CO column density estimate for the 65 km s^{-1} cloud near G49.5−0.4 is therefore presently impossible.

ii) *Gas at 50* km s^{-1}

The 6-cm line at 50 km s^{-1} becomes plainly visible and separate from the low-velocity wing of the 65 km s^{-1} line at positions about 30^s to the west of G49.5−0.4 (fig. 5*a*). The absorption line temperature at this velocity increases only slightly, if at all, in the direction of G49.5−0.4, so that the apparent optical depth (fig. 6*a*) reaches a minimum there. This behavior of the line temperature and apparent optical depth is just that expected if the cloud is situated behind G49.5−0.4 (§ II*a*).

Figure 8 shows equivalent width contours of the 50 km s^{-1} line over the region in which it is stronger than the low-velocity wing of the 65 km s^{-1} feature. Because the 50 km s^{-1} line probably originates from behind G49.5−0.4, the equivalent widths were calculated on the assumption that the cloud is absorbing only the cosmic background radiation (i.e., $T'_C = 0°$ K in eq. [1]). The presence of a diffuse galactic background, not included because of its uncertain intensity, would decrease the values of the contour levels but would not affect their shape. It is entirely possible that the source G49.4−0.3 is being absorbed by the 50 km s^{-1} cloud, but the difficulty of separating the radiation contribution of this source from G49.5−0.4 forced us to assume that both sources are in front of the cloud for calculation of the equivalent widths.

The position of maximum equivalent width[3] for the 50 km s^{-1} cloud lies only 3′ away from the H II region G49.4−0.3 whose recombination-line velocity is 52.8 km s^{-1} (Wilson *et al.* 1970); the cloud and this H II region are therefore probably close to each other. A good part of the 3′ discrepancy in positions can perhaps be accounted for by interference from the wings of the 65 and 57 km s^{-1} lines which are very strong in the direction on G49.5−0.4. Both the peak velocity and the mean velocity of the 50 km s^{-1} line are virtually constant over the region in which the line was detected.

The CO spectrum in the direction of G49.5−0.4 (fig. 9*a*) shows weak ($T_A \simeq 4°$ K) emission at 50 km s^{-1}. To the west of G49.5−0.4 (data not shown) the 57 km s^{-1} line weakens and the 50 km s^{-1} line becomes a distinct feature with a line antenna

[3] Also the position of maximum integrated line temperature since the W contours were calculated under the assumption of a constant background radiation.

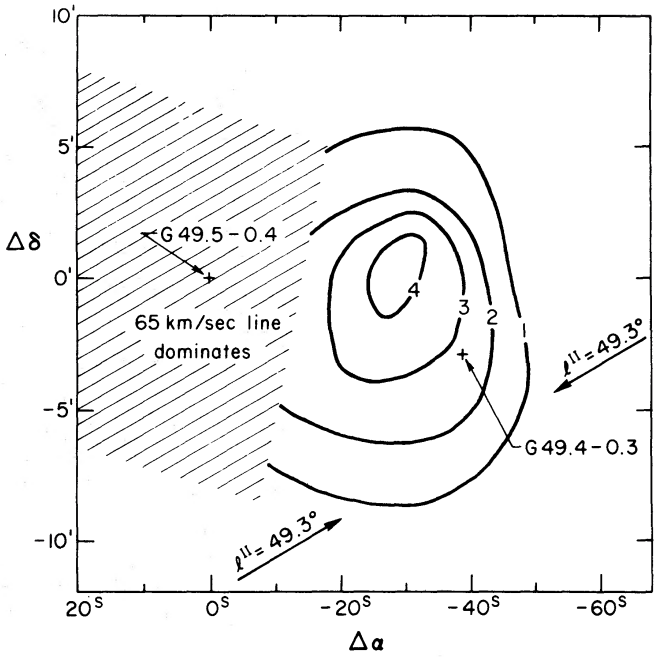

FIG. 8.—Contour diagram of equivalent width in the $(\Delta\alpha, \Delta\delta)$-plane for the 50 km s^{-1} H_2CO line in W51. $\Delta\alpha$ and $\Delta\delta$ are defined as in fig. 5*a*, and units of W are km s^{-1}. In the shaded region the wing of the 65 km s^{-1} line extends to low velocities and makes measurements of the 50 km s^{-1} line impossible. (W is calculated under the assumption that the cloud is located *behind* the continuum source; see § III*b*[ii].)

temperature of 8° K in the direction of G49.4−0.3. Because ^{13}CO observations do not extend to G49.4−0.3 and the H_2CO optical depths are uncertain, we forgo a quantitative comparison of the CO and H_2CO lines in this cloud.

iii) *Gas at 57* km s^{-1}

The 57 km s^{-1} gas (fig. 9*a*) shows up as the most intense feature in the mm emission spectra of CO, CN, HCN, H_2CO, and CS (Penzias *et al.* 1971*a*, *b*; Jefferts, Penzias, and Wilson 1970; Snyder and Buhl 1971; Thaddeus *et al.* 1971), but is only faintly visible in 6-cm H_2CO absorption. All of the 57 km s^{-1} millimeter lines have their peak emission occurring less than 1′ from the center of G49.5−0.4; and the half-intensity size of the CS and millimeter H_2CO emission region is 3′, approximately the size of the H II region. The case for close proximity of this gas to the H II region is made even more conclusive by the 58.2 km s^{-1} recombination-line velocity of the H II region.

The millimeter emission can be followed out much farther from the center of the H II region in the CO line than in the CS or millimeter H_2CO lines. Although the temperature of the CO line decreases away from the central direction of G49.5−0.4, the relative strength of the CO and ^{13}CO lines changes little from the value of 3 measured in the center out to 4′ away, the extent of the ^{13}CO observations. This apparent constancy of the CO opacity ($\sim$40, assuming a terrestial $^{12}C/^{13}C$ abundance ratio) and the observation of a 57 km s^{-1} 6-cm H_2CO line at a position $\sim$10′ away from the H II region (see below) once again suggests that, as in W49, the *apparent* size of the CO emission region is governed more by changes in the excitation temperature T_{01} than by the optical depth of the 2.6-mm line.

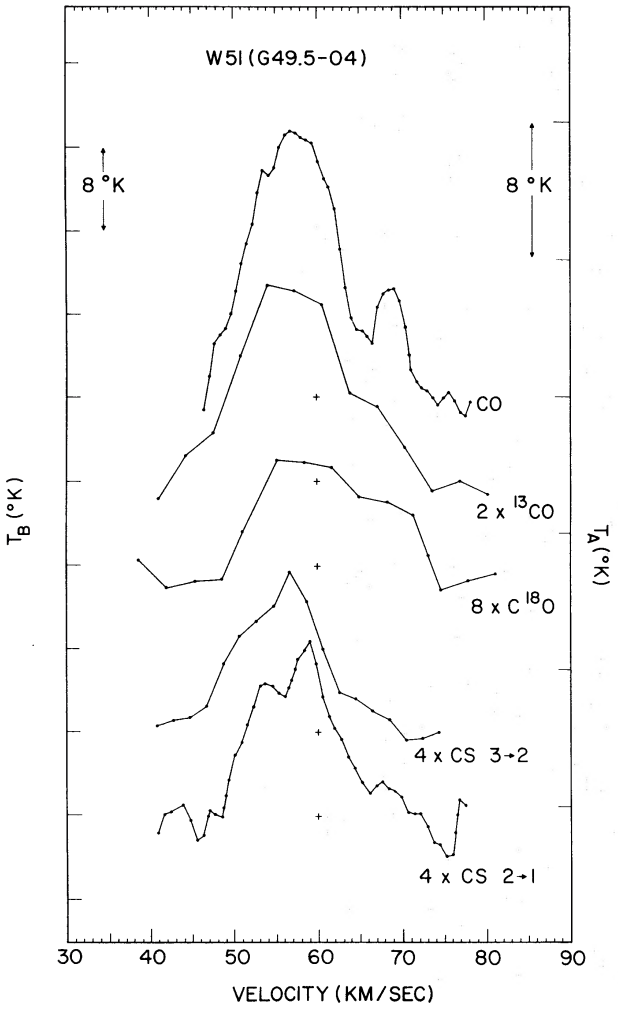

FIG. 9a

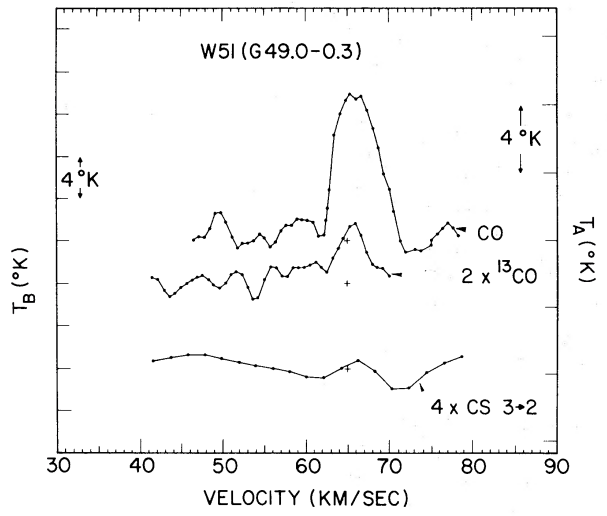

FIG. 9b

FIGS. 9a and 9b.—Spectra of CO, ^{13}CO, $C^{18}O$, CS ($J = 3 \rightarrow J = 2$), and CS ($J = 2 \rightarrow J = 1$) emissions in W51 at G49.5−0.4 and at G49.0−0.3. The vertical scale on the right is antenna temperature T_A, and that on the left is T_A/η ($\approx$ brightness temperature T_B, for $T_B > 10°$ K). Note that all spectra other than CO have been expanded vertically.

In most 6-cm spectra of W51 the 57 km s^{-1} line is severely blended with the much stronger 65 km s^{-1} line, but at about 6′ southeast of G49.5−0.4 it is quite distinct. There is no evidence of this line in either H_2CO or CO near the other W51 H II regions (see figs. 5*b* and 9*b*); therefore, although it is definitely near G49.5−0.4, the angular extent of the cloud is between 2 (CO observations) and 6 (H_2CO observations) times that of the H II region.

It is of interest to ask why this 57 km s^{-1} gas appears only faintly in H_2CO absorption spectra and yet produces the strongest line in the millimeter spectra. From the CO brightness temperature in figure 9*a*, we estimate that $T_{01} = 26°$ K, and that the $C^{18}O$ and ^{13}CO optical depths are 0.048 and 0.41. Using terrestrial isotope abundance ratios, the CO optical depth is between 24 and 36. The column density of CO through the center of this cloud is then $\sim 2 \times 10^{19}$ cm^{-2}. If the H_2CO/CO abundance ratio is $\sim 2 \times 10^{-5}$, then the column density N_1 of 1_{11} rotational state H_2CO molecules should be $\sim 10^{14}$ cm^{-2}. This corresponds to a 6-cm equivalent width of 6 km s^{-1}, and the *true* optical depth at the peak of the 6-cm line should be ~ 1. Although the CO observations indicate that the 57 km s^{-1} cloud has sufficient angular extent to fill the 6′ H_2CO beam, it is evident from figure 6*a* that the *apparent* optical depth at 57 km s^{-1} near G49.5−0.4 is only ~ 0.05. A most obvious explanation for this inconsistency is that the 57 km s^{-1} gas is located just behind G49.5−0.4 and is therefore not absorbing the radiation from this source. If this is so, then the H_2CO will be absorbing only the microwave background plus a small ($\leq 1°$ K) amount of diffuse galactic radiation. The absorption line temperature should then be $\sim 1°$ K—in good agreement with the observed value of 0.8° K at 57 km s^{-1} (fig. 5*a*).

Mass estimates for the 57 km s^{-1} molecular cloud may be obtained by integrating the CO column density over the cloud and assuming once again that all the carbon is bound up in CO. The minimum mass of the cloud is then $\simeq 10^5$ $M_\odot$, an estimate with a large uncertainty due to poor knowledge of the angular extent. This mass is 20 times that of the H II region G49.5−0.4 (table 1) and makes this one of the most massive clouds observed outside of the galactic center. The column density estimated from CO observations (6×10^{22} cm^{-2}) suggests a *minimum* gas density in the range 3×10^2 to 10^3 cm^{-3}.

IV. MOLECULAR REGIONS OF HIGH EXCITATION

In addition to the CO and H_2CO lines, we have looked for the $J = 2 \rightarrow 1$ and $3 \rightarrow 2$ transitions of CS (at 97.9810 and 146.9692 GHz) in W49 and W51.[4] The spontaneous rates of these transitions are 2.1×10^{-5} and 6.5×10^{-5} s^{-1}; they therefore pinpoint molecular regions with high excitation rates.

In both W49 and W51 the CS emission is strongly correlated with the positions of the H II regions. In W49A the $2 \rightarrow 1$ emission is seen at 12 km s^{-1} with a peak antenna temperature of 1.5° K, and drops to half-intensity less than 2′ away. The 12 km s^{-1} gas is also detected in the $3 \rightarrow 2$ transition with an approximate antenna temperature of 1° K, but our spectra are very noisy. In W51 the $2 \rightarrow 1$ and $3 \rightarrow 2$ emission comes principally from the 57 km s^{-1} gas (fig. 9*a*). The temperatures of both lines are nearly equal and are at half-intensity only 1′ away from G49.5−0.4. In the direction of G49.0−0.3 (fig. 9*b*) no CS $3 \rightarrow 2$ emission is seen corresponding to the fairly strong CO line at 66 km s^{-1}.

CS opacity estimates from isotope line strengths are difficult on account of the low CS intensities. The $C^{34}S$ $3 \rightarrow 2$ transition at 57 km s^{-1} has been detected at one-quarter the intensity of the CS line. If the terrestrial isotope ratio, $^{32}S/^{34}S$, of 25 holds for W51, then the $3 \rightarrow 2$ CS line is probably optically thick, and its brightness tem-

[4] An extensive survey and discussion of the CS lines will appear in Solomon *et al.* (1972*a*).

perature gives a good measure of the excitation temperature ($\sim 7.4°$ K [eq. (5a)]). If the $2 \rightarrow 1$ transition is also optically thick, its excitation temperature is 7.3° K. Similar low excitation temperature may exist in the HCN (Snyder and Buhl 1971) and 2-mm H_2CO (Thaddeus *et al.* 1971) transitions which also require high excitation rates in order to be excited above 2.7° K. In contrast, the CO excitation temperature, probably a lower limit to the gas kinetic temperature, is $\sim 26°$ K near the W51 peak.

Though they are excited well above the cosmic background near the H II regions, it is clear that the CS $3 \rightarrow 2$ and $2 \rightarrow 1$ transitions are not thermalized in any of the observed clouds. Moreover, the level of excitation appears to decrease away from the H II regions. Excitation by *electrons* in gas bordering the H II regions would explain the correlation between the high-excitation gas and H II regions; however, the mechanism maintaining a high electron density unfortunately would probably dissociate the molecules. Also because both the A's and the electron collision rates scale with the transition matrix element, electrons should excite CO and CS almost equally. At a kinetic temperature of 50° K, the observed CO excitation requires an electron density of $\sim 10^2$ cm^{-3}, 30 times greater than that needed for the CS.

If instead the observed brightness of the CS lines is provided *solely by collisions with neutral particles* (neglecting the photon scattering), then the gas density must be $\sim 6 \times 10^5$ and these densities must exist over a region comparable in area to the H II regions (~ 9 arcmin^2). It has been argued (Goldsmith 1972) that high excitation temperatures and even inversions can be produced by neutral particle collisions under conditions when multiquanta ($\Delta J > 1$) collisions have a strength equal to those of $\Delta J = 1$. However, this is true only in the limit of $\tau \ll 1$ since absorption of trapped photons depopulates excited states if $\tau \geq 1$. For CS the evidence from the isotopic lines as well as the relative strength of the 3–2 and 2–1 transitions (see Solomon *et al.* 1972*a*) indicates $\tau \gg 1$. Therefore, the excitation-temperature calculations of Goldsmith (1972) do not apply and the necessary neutral density estimated above must be regarded as approximately correct for the pure collision-dominated case. Such a high *neutral* particle density, unless only in a thin shell around the H II region or in small condensed objects, seems unlikely in view of the much lower average densities in the H II regions derived from radio continuum measurements and in view of the short dynamical timescales expected for such a dense and dusty gas.

The problems confronting models for the CS excitation which involve only collisions over a large volume suggest that the effects of radiative transfer should be considered more seriously. The near equality of the brightness temperatures in the two CS lines at different frequencies is suggestive of an optically thick medium at a temperature much greater than $h\nu/\kappa$. Thus the observed CS line radiation could be scattered radiation from compact, high-temperature objects which are much smaller than the apparent size of the CS emission region. The compact sources could be dense regions in which the CS is thermalized at a high temperature. High pressures in or on the border of the H II regions would be conducive to the compression of the neutral gas to a high density and thus explain the general correlation of the CS intensities with the H II regions. These high-density molecular regions may be protostars or protoclusters which will become compact H II regions after the formation of massive stars. Very dense ($n_e > 10^4$ cm^{-3}) knots of ionized gas observed in both W49 and W51 (§ I) may represent a later evolutionary phase of dense molecular regions.

Therefore, although the observed excitation in the transitions of CS (and similar molecules) well above the cosmic background implies a very high neutral gas density ($\geq 10^5$ cm^{-3}) somewhere in the cloud, we feel that such is probably not required over the full angular extent of the CS emission region. It would then be erroneous to conclude that this high density was typical of the whole cloud and to derive a mass estimate from it.

V. CONCLUSIONS

1. Five of the seven observed clouds (3 and 14 km s^{-1} in W49A, and 50, 57, and 65 km s^{-1} in W51) are associated with one or more of the H II regions and show moderately broad lines (4 km $s^{-1} \lesssim \Delta V \lesssim$ 15 km s^{-1}). The 65 km s^{-1} cloud in W51 extends over a region containing at least three H II regions, and appears as a self-absorption feature in the CO spectrum of G49.5−0.4. The two other clouds (39 and 62 km s^{-1} in W49A) show narrow H_2CO lines and are probably dark nebulae unrelated to any H II regions.

2. For three of the five clouds we have estimated the masses and find them to be in the range 10^4–10^5 $M_\odot$. *These masses, almost certainly minimum values, are more than 10 times those of the associated* H II *regions* and only a little less than the masses of some molecular clouds in the galactic center.

3. The 3 and 14 km s^{-1} clouds in W49A appear to be approaching this H II region at velocities of $\sim$5 km s^{-1}. The CO observations suggest that the gas *kinetic* temperature in the 14 km s^{-1} cloud is highest near the H II region.

4. The 6-cm H_2CO observations of three molecular clouds which also have intense millimeter emission lines (3 and 14 km s^{-1} in W49A, and 57 km s^{-1} in W51) indicate that these clouds are considerably more extensive than either the associated H II regions or the half-intensity sizes determined from the millimeter-line observations. Some of the millimeter emission lines, especially those of CS, show a strong correlation of their intensities with the positions of H II regions.

5. Determination of the excitation temperature in the H_2CO 6-cm transition from the two narrow lines in the direction of W49 yields $T_{12} = 1.76° \pm 1.2°$ K.

We thank R. Taam for assistance with the H_2CO observations and L. B. Lucy for comments on an earlier version of this paper.

REFERENCES

Allen, C. W. 1963, *Astrophysical Quantities* (2d ed.; London: Athlone Press).
Buhl, D., Snyder, L. E., Schwartz, P. R., and Barrett, A. H. 1969, *Ap. J.* (*Letters*), **158**, L97.
Goldsmith, P. F. 1972, *Ap. J.*, **176**, 597.
Gordon, M. A., and Wallace, D. C. 1971, *Ap. J.*, **167**, 235.
Goss, W. M., and Shaver, P. A. 1970, *Australian J. Phys., Ap. Suppl.*, **14**, 1.
Heiles, C. 1972, *NRAO Symposium on Interstellar Molecules, October 1971*, ed. M. A. Gordon (New York: John Wiley & Sons) (in press).
Jefferts, K. B., Penzias, A. A., and Wilson, R. W. 1970, *Ap. J.* (*Letters*), **161**, L87.
Kutner, M., Scoville, N. Z., Solomon, P. M., and Thaddeus, P. 1973 (in preparation).
Mezger, P. G., and Henderson, A. P. 1967, *Ap. J.*, **147**, 471.
Mezger, P. G., Schraml, J., and Terzian, Y. 1967, *Ap. J.*, **150**, 807.
Miley, G. K., Turner, B. E., Balick, B., and Heiles, C. 1970, *Ap. J.* (*Letters*), **160**, L119.
Palmer, P., Zuckerman, B., Buhl, D., and Snyder, L. E. 1969, *Ap. J.* (*Letters*), **156**, L147.
Penzias, A. A., Jefferts, K. B., Liszt, H., Wilson, R. W., and Solomon, P. M. 1972*a* (in preparation).
Penzias, A. A., Jefferts, K. B., and Wilson, R. W. 1971*a*, *Ap. J.*, **165**, 229.
Penzias, A. A., Solomon, P. M., Jefferts, K. B., and Wilson, R. W. 1972*b*, *Ap. J.* (*Letters*), **174**, L43.
Penzias, A. A., Solomon, P. M., Wilson, R. W., and Jefferts, K. B. 1971*b*, *Ap. J.* (*Letters*), **168**, L53.
Raimond, E., and Eliasson, B. 1969, *Ap. J.*, **155**, 817.
Reifenstein, E. C., Wilson, T. L., Burke, B. F., Mezger, P. G., and Altenhoff, W. J. 1970, *Astr. and Ap.*, **4**, 357.
Rogers, A. E., Moran, J. M., Crowther, P. P., Burke, B. F., Meeks, M. L., Ball, J. A., and Hyde, G. M. 1966, *Phys. Rev. Letters*, **17**, 450.
Schraml, J., and Mezger, P. G. 1969, *Ap. J.*, **156**, 269.
Scoville, N. Z., Solomon, P. M., and Thaddeus, P. 1972, *Ap. J.*, **172**, 335.
Shaver, P. A. 1969, *M.N.R.A.S.*, **142**, 273.
Snyder, L. E., and Buhl, D. 1971, *Ap. J.* (*Letters*), **163**, L47.
Solomon, P. M., Jefferts, K. B., Penzias, A. A., Wilson, R. W., and Liszt, H. 1972*a* (in preparation).

Solomon, P. M., Scoville, N. Z., Jefferts, K. B., Penzias, A. A., and Wilson, R. W. 1972*b*, *Ap. J.* (in press).
Solomon, P. M., and Werner, M. W. 1971, *Ap. J.*, **165**, 41.
Thaddeus, P., Wilson, R. W., Kutner, M., Penzias, A. A., and Jefferts, K. B. 1971, *Ap. J.* (*Letters*), **168**, L59.
Tucker, K. D., Tomasevich, B. R., and Thaddeus, P. 1971, *Ap. J.* (*Letters*), **161**, L153.
Weaver, H., Dieter, N. H., and Williams, D. R. W. 1969, *Ap. J. Suppl.*, **16**, 219.
Westerhout, G. 1958, *B.A.N.*, **14**, 215.
Whiteoak, J. B., and Gardner, F. F. 1970, *Ap. Letters*, **5**, 5.
Wilson, T. L., Mezger, P. G., Gardner, F. F., and Milne, D. K., 1970, *Ap. Letters*, **5**, 99.
Wynn-Williams, C. G. 1969, *M.N.R.A.S.*, **142**, 453.
Zuckerman, B., Buhl, D., Palmer, P., and Snyder, L. E. 1970, *Ap. J.*, **160**, 485.